

Broadband Simplified SAR Measurement Method Using Solid Material

Keita Ochiyama¹, Naobumi Michishita¹, Yoshihide Yamada¹,
Hiroyuki Arai², and Toshiyasu Tanaka³

¹Department of Electrical and Electronic Engineering, National Defense Academy

²Yokohama National University ³Microwave Factory Co., Ltd.

naobumi@nda.ac.jp

1. Introduction

Simplification of the spatial specific absorption rate (SAR) measurement method is required for mobile devices used near the human body. A simplified SAR measurement method using a lightweight phantom comprising a wave absorber has been proposed as an alternative to a liquid or solid phantom at 1,850 MHz [1]. An electric field probe is embedded in the wave absorber phantom, and is scanned with the phantom in two dimensions. The peak spatial-average SAR is estimated by using only one observation layer in the wave absorber phantom. The validity of the proposed measurement method is verified through the standard measured results of the local SAR at 835 MHz and 1,950 MHz [2]. Since the wave absorber has stable electrical parameters and low density, the phantom is easy to handle and lightweight. However, the amplitude error of the surface impedance of the wave absorber and liquid phantoms are not acceptable in high frequency band. To achieve the broadband measurement method, this paper presents the design of the broadband phantom composed of the solid material at from 300 MHz to 6 GHz. The electrical parameters and the size of the phantom are clarified through the electromagnetic simulation.

2. Design of broadband solid phantom

Figure 1 shows the liquid phantom and the broadband solid phantom. In the simplified SAR measurement method, the internal electric field distribution in the liquid phantom is estimated by using the surface electric field on the solid material. Therefore, the surface electric field E_{sol} of the solid phantom should be identical to E_{liq} of the liquid phantom.

2.1 Electrical parameters of phantom

Figure 2 shows the electrical parameters at from 3 GHz to 6 GHz. The symbol ● represents the electrical parameters of the actual wave absorber. Each line is the electrical parameters that are equal to the surface electric field on the liquid phantom. The relative permittivity and conductivity of the actual wave absorber are low at the frequency more than 4 GHz. Therefore, the conventional wave absorber phantom cannot be used in high frequency band. Each line is also divided by two regions. The solid lines indicate the feasible electrical parameters of the solid material [3]. The electrical parameters of the dashed lines cannot be achieved by using the solid material. Since the solid material can achieve high permittivity and low conductivity, the surface electric field at each frequency is identical by selecting the electrical parameters ($\epsilon' = 40$ and $\sigma = 1.4$) represented as the symbol ○. The electrical parameters can be obtained by using the solid material composed of the ceramic powder of 45%, graphite of 2% and resin of 53%. The permittivity and conductivity of the ceramics composed of barium titanate are 20 and 0.02 [3]. Figure 3 shows the electrical parameters at from 300 MHz to 3 GHz. The symbol ● represents the electrical parameters of the actual wave absorber. Each line is the electrical parameters that are equal to the surface electric field on the liquid phantom. The symbol ● is close to the line at each frequency, the wave absorber can be used as the phantom in the conventional simplified SAR measurement method in [1], [2]. When the

symbol \circ is also selected as the electrical parameters in low frequency band, the surface electric field is almost identical at from 300 MHz to 6 GHz.

2.2 Size of phantom

Figure 4 shows the simulation model of an infinitesimal dipole antenna near solid material at 300 MHz. The distance of the antenna and the solid material is 15 mm. Figure 5 shows the maximum surface electric field intensity when L , W , and T are varied. When one parameter is varied, other parameters are large enough. Figure 5 shows the maximum surface electric field intensity when L , W , and T are varied. The dimensions of the solid material are decided as $L \times W \times T = 225 \times 150 \times 100$ mm.

3. Electric field distributions of handset antennas

Figure 6 shows the simulation model of an antenna under test (AUT) near solid material with $L \times W \times T = 225 \times 150 \times 100$ mm. Figure 7 shows the configuration of a helical antenna mounted on a metal plate at 300 MHz. A tap feeding structure is used for achieving impedance matching. The number of turns is 58. The diameter of the helical antenna is 3 mm. The radius of the wire is 0.15 mm. The distance of the antenna and the solid material is 15 mm. Figure 8 shows the configuration of an inverted-F antenna mounted on a metal plate at 6 GHz. The radius of the wire is 0.5 mm. The distance of the antenna and the solid material is 10 mm. Figure 9 shows surface electric field distributions of the liquid phantom and the solid material at 300 MHz. The maximum electric field is observed under the connection part between the tap and the helical antenna. In addition, large electric field is distributed under the antenna. The error of the maximum electric field intensity is 2.4%. Figure 10 shows surface electric field distributions of the liquid phantom and the solid material at 6 GHz. The maximum electric field is observed under the feeding point. Another large electric field is confirmed at opposite side of the feeding point in the upper part of the metal plate. Also, the other several peaks are confirmed along the longitudinal of the metal plate. The error of the maximum electric field intensity is 1.3%.

4. Conclusion

This paper investigates the broadband solid phantom for the simplified SAR measurement method at from 300 MHz to 6 GHz. The electric parameters and dimensions of the solid material are $\epsilon' = 40$, $\sigma = 1.4$ and $L \times W \times T = 225 \times 150 \times 100$ mm, respectively.

References

- [1] N. Michishita, T. Watanabe, Y. Yamada, H. Arai, and T. Tanaka, "Simplified local specific absorption rate measurement method using lightweight phantom composed of wave absorber embedded of electric field probe," *IEEE Trans. Electromagn. Compat.*, vol.54, no.1, pp.181-187, Feb. 2012.
- [2] K. Ochiyama, N. Michishita, Y. Yamada, H. Arai, and T. Tanaka "Simplified measurement of specific absorption rate for handset antennas by using broadband wave absorber phantom," *EMC Europe*, Rome, Italy, Sept. 2012, to be presented.
- [3] T. Kobayashi, T. Nojima, "Simulation of Electromagnetic Properties of Biological Tissues with Solid and Liquid Materials and Its applications," *IEICE Tech. Report*, MW92-35, pp.31-38, May 1992.

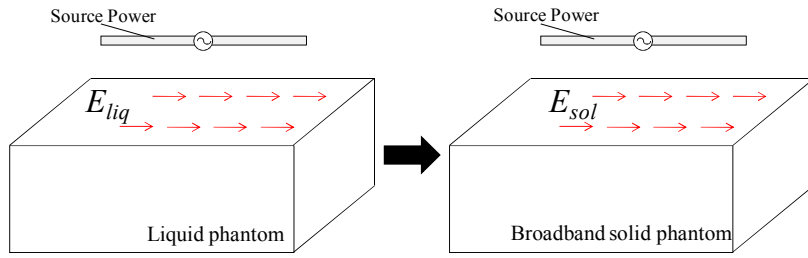


Figure 1: The liquid phantom and the equivalent broadband solid phantom

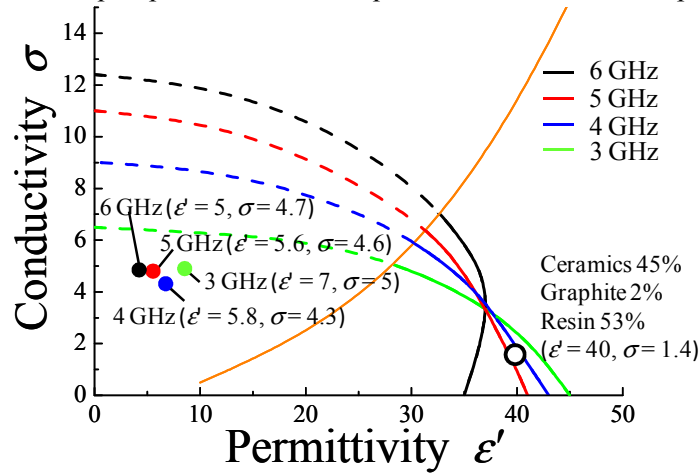


Figure 2: Electrical parameters that is equal to surface electric field of liquid phantom at high frequency band

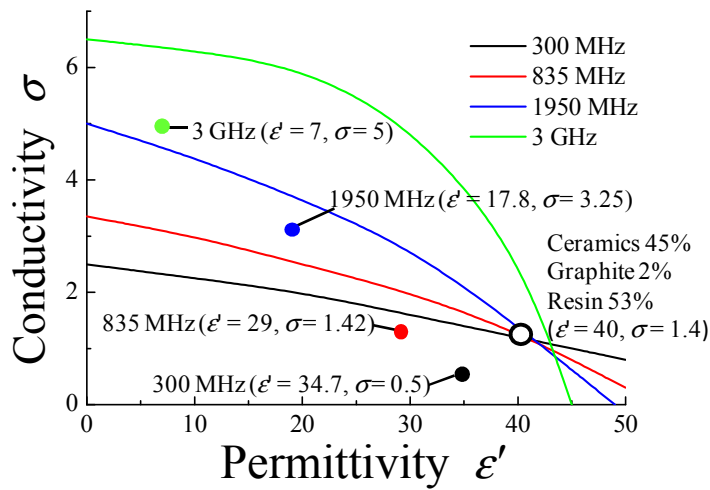


Figure 3: Electrical parameters that is equal to surface electric field of liquid phantom at low frequency band

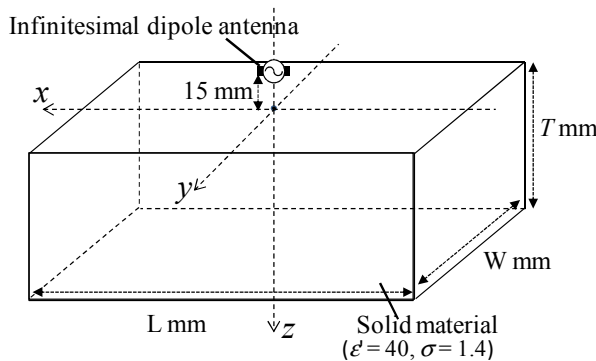


Figure 4: Simulation model of infinitesimal dipole near solid material

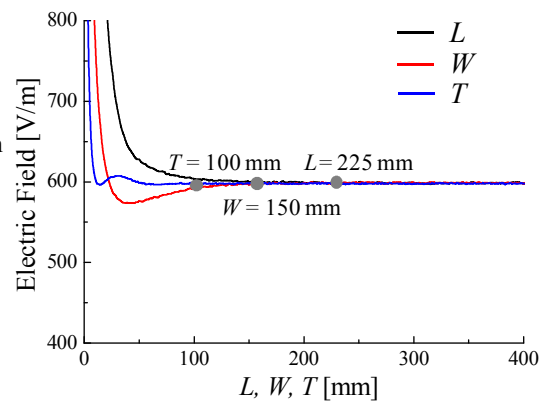


Figure 5: The maximum surface electric field when L , W and T are varied at 300 MHz.

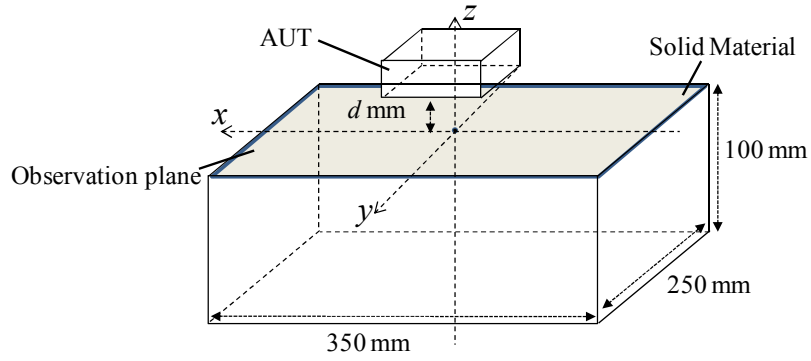


Figure 6: Simulation model of AUT near solid material

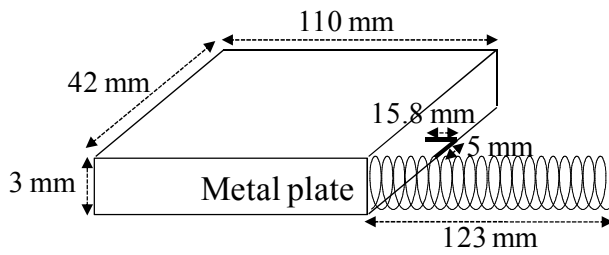


Figure 7: Configuration of helical antenna on metal plate (300 MHz)

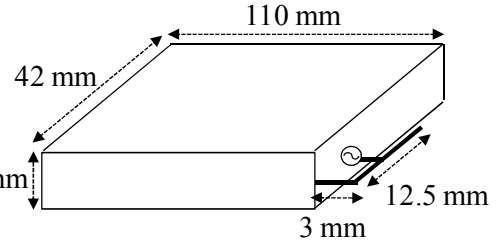
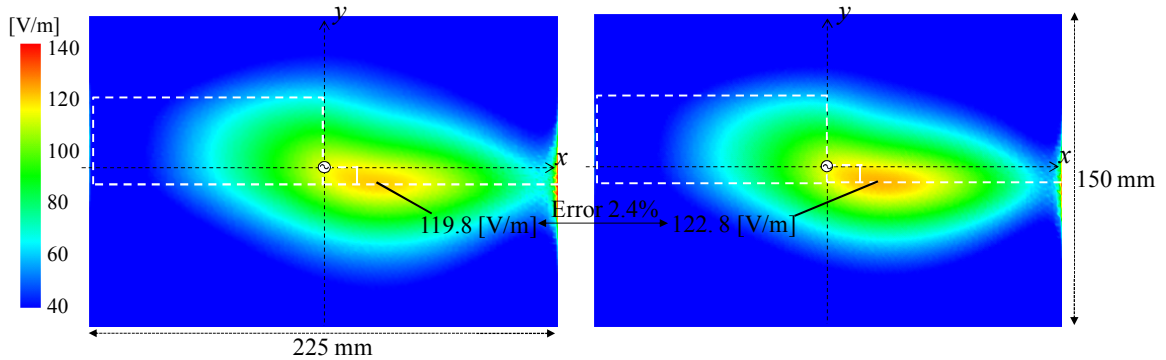
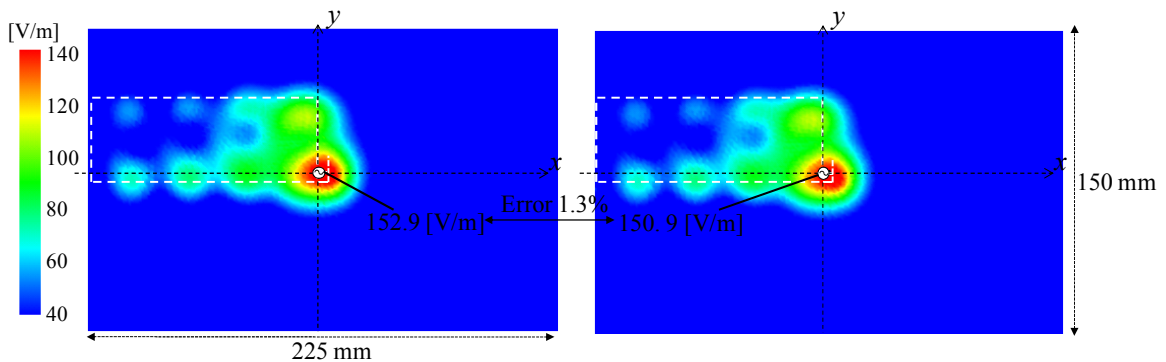


Figure 8: Configuration of inverted-F antenna on metal plate (6 GHz)



(a) Liquid phantom (b) Solid material
Figure 9: Surface electric field distributions at 300 MHz



(a) Liquid phantom (b) Solid material
Figure 10: Surface electric field distributions at 6 GHz